

# Tidal Effect of Modified Schwarzschild Black Hole Under the Influence of Rindler Acceleration and Cosmological Constant

R. Minhas<sup>1\*</sup>, M. U. Hashmi<sup>1</sup>, and M. Ali<sup>1</sup>

<sup>1</sup>Department of Basic Sciences, Superior University, Lahore, 54000, Pakistan.

\*Corresponding Author: R. Minhas. Email: rashidminhas544@gmail.com

Received: June 11, 2024 Accepted: September 29, 2024

**Abstract:** We study the effects of tidal force and the behavior of the geodesic deviation vector in the background of a modified Schwarzschild black hole. In this analysis, we obtain the curvature tensor on a tetrad basis to evaluate the radial and angular tidal force on a radially free-falling particle towards a black hole. The radial tidal forces increase with an increase in the  $\Lambda$  (cosmological constant) value but decrease when the value of  $r$  increases. The variation of angular tidal force for  $\Lambda$  shows increasing behavior and gradually decreases to a smooth curve when increasing the radius. We solve the geodesic deviation equation numerically and analyze how the geodesic separation vector varies with radial coordinates for two neighboring geodesics under suitable initial conditions. All the obtained results are tested for a modified Schwarzschild black hole by constraining the value of the acceleration parameter and the cosmological constant. The results are also compared with a simple Schwarzschild black hole.

**Keywords:** Black Holes; Rindler Acceleration; Geodesic Deviation Equation; Tidal Force.

## 1. Introduction

In general relativity, black holes (BHs) are generated when stars with masses similar to or greater than the sun's mass collide under their gravitational field. Einstein's theory of relativity characterizes the BH as an area of space with many objects that can escape the gravitational field. The BH is the most significant gravitationally massive object identified in active galaxies.

Black holes are regarded as outdoor research facilities where we may test our knowledge of nature. Although BHs initially developed theoretically, subsequent advancements in the subject continue to improve their ability to observe scientific reality rather than fantasy. Studying BHs' physical features becomes one of the most important first steps in this direction since they give us the natural framework to evaluate and improve the existing scientific understanding of gravity. More than a century has passed since BHs were proposed as the theoretical answer to Einstein's field equations. General relativity (GR) is widely regarded as the most comprehensive theory of gravity [1]. On the experimental side, all findings on the cosmic scale point to the presence of dark matter and dark energy [2]-[6], suggesting that GR is flawed at this size.

After that, gravitational experiments on submillimeter scales [7, 8], in the solar system [9]-[15], in binary-pulsar systems [16]-[20], and on celestial and cosmic scales [21]-[24] have shown that Einstein's theory is incredibly accurate. The initial identification of gravitational waves provided an entirely novel tool for testing gravity in high-gravity conditions. The currently detected gravitational waves, as projected by GR, can only be formed by intense gravitational forces and barely interact with matter, carrying information concerning the characteristics of gravity in strong fields' domain of expertise. The curvature is important in GR for understanding the geometric impact of curved spacetime. The study of geodesics and their deformations in

the context of a specific spacetime is a beautiful approach to the Pioneer spacecraft [29]. However, at great distances, the force law that Rindler's acceleration term produces significantly impacts gravity. Furthermore, Turyshev et al. [30] have researched an alternate explanation for the Pioneer anomaly to Grumiller's changed gravity: the satellites' thermal heat loss. However, RMSBH may theoretically explain changes in planetary orbits during perihelion, gravitational redshift, and spiral galaxy rotation curves. Ref [31] gives a quantum gravity theory's Rindler acceleration, which may be used to clarify why the nearby galaxies' curves are spinning.

We investigated the new Rindler acceleration term as a substitute for dark matter in galaxies. The HI nearby Galaxy Survey confirms that in the end, giving a Rindler acceleration value of around  $a \approx 3 \times 10^{-99} \text{cm/s}^2$  [32]-[35]. Refs. [36, 37] provide research on tunnelling entropy and spectroscopy of RMSBH. Sakalli et al. have conducted research on light deflection and Hawking radiation for RMSBH recently [38].

Extreme gravitational fields around BHs can bend objects, causing phenomena like gravitational lensing and the bending of light trajectories due to spacetime's curvature. Tidal forces may amplify these effects, making gravitational lensing more noticeable. Investigating tidal events near BHs provides important information on the characteristics of these mysterious objects, how they affect the environment, and how matter accretes onto them. Tidal disruption and other tidal effect observations advance our knowledge of BH demography, feeding processes, and galaxy development.

Tidal phenomena are prominent in the cosmos and essential to astronomical circumstances like tidal disruption incidents. The gravitational field causes a body's shape to be warped, and this fluctuation in gravitational attraction between two locations is what causes the tidal force. In Schwarzschild spacetime, a body falling close to the event horizon suffers radial stretching and rotational compression [39]-[41]. It is shown that the location of the body and its charge-to-mass ratio is the tidal effect in Reissner-Nordström spacetime throughout this paper, we examine the tidal forces and their impact on a dark matter surrounded cosmological constant. New studies on the timelike and null geodesics around this BH spacetime have shown how the presence of dark matter around the cosmological constant changes the structure of the related geodesics. We chose to investigate the tidal forces and the development of vectors of geodesic deviation within this BH metric in order to identify these distinctive features. To investigate the geodesic deviation vector behaviour and search for potential impacts of the many factors involved, we created generalized equations for geodesic deviation and resolved them. This is the manner in which the article is structured: In Section 2, we examine the RMSBH and the geodesic motion of this BH with the effects of Rindler acceleration and the cosmological constant. In Section 3, we explored in detail the geodesic deviation equations as well as tidal forces for neutral.

All authors have same contribution.

## 2. Radial Geodesics in Rindler Modified Schwarzschild Black Hole

This section will cover Rindler's modified Schwarzschild black hole's geometry. Grumiller [58] developed an effective model, often referred to as RMSBH geometry, for the gravity of a central object at an enormous scale beyond the galaxy. Test particle geodesics exhibit an abnormal acceleration due to the Rindler term's existence in the RMSBH spacetime. The action of RMSBH is given as

$$S = - \int d^2x \sqrt{-g} [R\Phi^2 + 2(\partial\Phi)^2 + 8\Phi\alpha - 6\Phi\Lambda + 2]$$

Where  $\alpha$  represents the Rindler acceleration [59], which is really missing in Einstein's GR,  $g = \det(g_{\mu\nu})$  is metric tensor, scalar field  $\Phi$ ,  $\Lambda$  indicates the cosmological constant, and Ricci scalar  $R$ . Finally, the static spherically symmetric RMSBH spacetime may be shown by considering the action, Eq. (1), and addressing the field equations with a cosmological constant

$$ds^2 = -G(r)dt^2 + \frac{dr^2}{G(r)} + r^2(d\theta^2 + \sin^2\theta d\phi^2),$$

With

$$G(r) = 1 - \frac{2M}{r} + 2ar - \Lambda r^2,$$

Where M representing the BH mass, the Schwarzschild solution may be readily recovered when  $a = \Lambda = 0$ . Furthermore, Eq. (2) simplifies to the two-dimensional Rindler metric [60] if  $\Lambda = M = 0$ , above (Eq.3). Based on [61], the value of  $\Lambda$  is estimated to be  $10^{-123}$ . For convenience, one may thus set it  $\Lambda = 0$ , but, to have a more generic answer, we shall not do so in the current research. The Rindler acceleration is significant because, when  $a$  is treated as a positive parameter, it implies a continuous acceleration towards the source and may be used to determine the form of the galactic rotation curve. In [58], the author also says that the "Rindler acceleration" might explain the "Pioneer anomaly," which is an apparent radial constant acceleration of order  $a \approx 10^{-11} \text{m/s}^2$  that is linked to the paths of the Pioneer spacecraft. [62]. This is because the cosmological constant term  $\Lambda r^2$  and the Rindler term  $2ar$  become more important as distances get larger, up to the Hubble length, and get close to unity for  $a \approx 10^{-10} - 10^{-11} \text{m/s}^2$ . According to [63], the Pioneer acceleration and the modified Newtonian dynamics characteristic acceleration have the same value. It is important to note that using this gravity model that accounts for effective dilation scalar fields, the Rindler acceleration  $a$  is system-independent.

We shall now talk about the RMSBH's event horizon. If  $G(r) = 0$ , then a BH's event horizon radius  $r_+$  may be computed. Curiously, the calculation shows that just one of the three possible roots of  $r$  turns into the actual positive root, giving us the physical radius of the RMSBH horizon. The actual beneficial root emerges as

$$r_+ = \frac{2a}{3A\Lambda} - \frac{\sqrt[3]{2}(3\Lambda + 4a^2)}{3A\Lambda} - \frac{A}{3\sqrt[3]{2}\Lambda}.$$

In which

$$A = \sqrt[3]{54M\Lambda^2 - 16a^2 - 18a\Lambda + \sqrt{4(-4a^2 - 3\Lambda) + 54M\Lambda^2 - 16a^2 - 18a\Lambda}}.$$

It is seen that, as predicted, we get  $r_+ = 2M$  in the limits  $\Lambda \rightarrow 0$  and  $a \rightarrow 0$ .

The explicit analysis of radial geodesic motion in RMSBH is shown in Eq. (2), here  $ds = d\tau$  is used in Eq.(2)

$$G(r)\dot{t}^2 - G(r)^{-1}\dot{r}^2 = 1,$$

Where prime represents the differentiation w. r. t. the proper time  $\tau$ . To calculate the radial geodesic motion of test particles in RMSBH. We substitute  $ds = d\tau$  in Eq. (1) and consider the angular motion

$$\frac{d\theta}{d\tau} = \frac{d\phi}{d\tau} = 0,$$

then we get

$$\left(\frac{dr}{d\tau}\right)^2 = E^2 - G(r),$$

$$\boxed{E = G(r)\frac{dt}{d\tau}}$$

The energy of the test particle is preserved and converted. Suppose that the test particle is at rest in the radial position  $r = b$ , we can estimate its energy via Eq. (3) which implies that the test particle radial acceleration is

$$A^R = -\frac{M + ar^2 - \Lambda r^3}{r^2}$$

$$E = \sqrt{G(r = b)}$$

The Newtonian radial acceleration  $A^R$  gives us Rindler-modified SBH "exerts" of massive test bodies on a neutral free fall. The Newtonian radial acceleration depends on the  $M$ ,  $a$  and  $\Lambda$  parameters, which increase with these values. It is consequently critical to observe that the test particle rests on a neutral body at  $r = b > r_+$ . The relativistic effect in Eq. (8) is expressed purely. It is crucial to note that the test particle would bounce back at  $r = b > r_+$  from rest on a neutral body  $R^{\text{stop}}$ . The radius  $R^{\text{stop}}$  can readily be determined as a root of

$$E^2 - G(r)$$

$$R^{\text{stop}} = \frac{(2ab - b^2\Lambda) \pm \sqrt{8Mb\Lambda + (b^2\Lambda - 2ab)^2}}{2b\Lambda}$$

The  $R^{\text{stop}}$  behaves like other BHs. The geodesic equation of motion is a key equation in general relativity that explains particle motion in curved spacetime. It is based on the extremal action principle, which states that a particle's precise path between two locations in spacetime is the path that extremizes an action. The mathematical formula for the geodesic equations in four velocities is

$$\frac{dv^0}{dt} + \frac{M + ar^2 - \Lambda r^3}{r^2 - 2Mr + 2ar^3 - \Lambda r^4} v^0 v^1 =$$

$$\frac{dv^1}{dt} + \frac{(M + r^2(a - 2\Lambda r))(r + 2ar^2 -}{r^3}$$

$$+(2M - r - 2ar^2 - \Lambda r^3)[(v^2)^2 + \sin^2$$

$$\frac{dv^2}{dt} + \frac{1}{r} v^1 v^2 - \sin \theta \cos \theta (v^3)^2 = 0,$$

$$\frac{dv^3}{dt} + \frac{1}{r} v^1 v^3 - \cot \theta v^2 v^3 = 0.$$

$$v^\mu = \frac{dx^\mu}{dt}$$

$$v^0 = \frac{\sqrt{r}C_1}{\sqrt{2M - r - 2ar^2 + \Lambda r^3}}, v^3 = \frac{C_2}{r^2},$$

To simplify and arrive at the outcome, we take into consideration geodesics in the equatorial plane as  $\theta = 90^\circ$ , and

Then, we obtain respectively, where  $C_1$  and  $C_2$  are constants of integration. The conserved quantities of energy and momentum of test particle by using the killing vectors  $\xi^\mu = (1, 0, 0, 0)$  and  $\eta^\mu = (0, 0, 0, 1)$  are given by

$$E = \left(1 - \frac{2M}{r} + 2ar - \Lambda r^2\right)v^0, L = r^2 v^3.$$

Comparing the above relations with Eqs. (14), we can fix the constants of integration as  $C_1 = E$ ,  $C_2 = L$  in the term of conserved quantities of E and L. Finally, by considering  $ds^2 = -kd\tau^2$  in Eqs. (1) and using Eqs. (14), one can obtain

$$v^1 = \pm \left[ E^2 - \left( K + \frac{L^2}{r^2} \right) \left( 1 - \frac{2M}{r} + 2ar - \Lambda r^2 \right) \right]^{\frac{1}{2}}$$

Where the - sign shows the inward and + outward motion of the particle, as well as a time-like (1) and null-like (0).

$$v^1 = \frac{dr}{d\tau} \quad v^2 = \frac{d\theta}{d\tau} = 0$$

### 3. Tidal force and geodesic deviation in Modified Schwarzschild Black Hole

The gravitational attraction on distinct regions of an object gets increasingly divergent as it approaches a BH. The side closest to the BH has a greater gravitational pull than the side farther away. This difference in gravitational force produces tidal force, which either stretches or compresses the item. Tidal forces cause the separation or spreading apart of initially parallel geodesics (i.e., the paths taken by freely falling objects). In the presence of a BH, tidal forces can cause neighboring geodesics to diverge or converge, changing their relative positions over time. The general equation of geodesic deviation [65, 66] is following:

$$e_{\hat{a}}^{\hat{\lambda}} e_{\hat{\lambda}\hat{\rho}} = \eta_{\hat{a}\hat{\rho}}$$

$$\eta^{\hat{\lambda}} = e_{\hat{a}}^{\hat{\lambda}} \eta^{\hat{a}}$$

The separation vector may be expressed as having a fixed value  $\eta^0 = 0$  [64]. The non-vanishing components of curvature tensor in the context of tetrad basis:

$$R_{10\hat{1}}^0 = \frac{G''(r)}{2}, R_{20\hat{2}}^0 = R_{30\hat{3}}^0 = R_{2\hat{1}\hat{2}}^1 = R_{3\hat{1}\hat{3}}^1 = \frac{G'(r)}{2r}, R_{10\hat{1}}^0 = \frac{1-G(r)}{r^2}.$$

Tidal forces in the neutral body therefore can be obtained as

$$\frac{d^2 \eta^{\hat{1}}}{d\tau^2} = \left( \frac{2M}{r^3} + \Lambda \right) \eta^{\hat{1}},$$

$$\frac{d^2 \eta^{\hat{i}}}{d\tau^2} = \left( \Lambda - \frac{2M}{r^3} - \frac{a}{r} \right) \eta^{\hat{i}},$$

Where  $i = 2, 3$ .

The variation of radial tidal force with the  $\Lambda$  parameter is shown in Fig. 1. The radial tidal forces increase with the value of  $\Lambda$  but show a decreasing curve to smooth the path along a radial direction. From Fig. 2, the variation of angular tidal force concerning  $\Lambda$  (cosmological constant) shows increasing behaviour and gradually decreases to a smooth curve when expanding the radius. Fig. 3 indicates that the angular tidal force sharply decreases with an increase in the value of  $a$ , and the tidal forces compress in an angular direction until  $r \rightarrow \infty$ .

$$\frac{D^2 \eta^{\hat{i}}}{D\tau^2} + R^{\lambda}_{\rho\sigma} v^{\rho} v^{\sigma} v^{\hat{i}} = 0,$$

Where  $R^{\lambda}_{\rho\sigma}$  is the Riemann curvature tensor, separation four-vectors  $\eta^{\lambda}$  and unit vector  $v^{\sigma}$  in geodesic. We present a tetrad basis for characterizing a neutral body, which is given as

$$e_0^{\lambda} = \left( \frac{E}{G(r)}, -\sqrt{E^2 - G(r)}, 0, 0 \right), e_1^{\lambda} = \left( \frac{-\sqrt{E^2 - G(r)}}{G(r)}, E, 0, 0 \right),$$

$$e_2^{\lambda} = (0, 0, 1, 0) \frac{1}{r}, e_3^{\lambda} = (0, 0, 0, 1) \frac{1}{r \sin \theta}.$$

Furthermore, solve the above Eqs. (19) and (20) in the context of radial coordinate  $r$  by using the expression We assume the test particle moves in a neutral, free fall towards the RMSBH. So, we get

$$\frac{dr}{d\tau} = -\sqrt{E^2 - G(r)}.$$

$$[E^2 - G(r)] \frac{d^2 \eta^{\hat{1}}}{dr^2} - \frac{G'(r)}{2} \frac{d\eta^{\hat{1}}}{dr} + \frac{G''(r)}{2} \eta^{\hat{1}} =$$

$$[E^2 - G(r)] \frac{d^2 \eta^{\hat{i}}}{dr^2} - \frac{G'(r)}{2} \frac{d\eta^{\hat{i}}}{dr} + \frac{G'(r)}{2r} \eta^{\hat{i}} =$$

which implies that the Eqs.(23)

$$\eta^{\hat{1}} = \sqrt{[E^2 - G(r)]} (D_1 + D_2 \int \frac{dr}{(E^2 - G(r))^{\frac{3}{2}}}) = 0,$$

and (24) is

$$\eta^{\hat{i}} = r (D_1 + D_2 \int \frac{dr}{r^2 \sqrt{(E^2 - G(r))}}) = 0.$$

The analytical solution to the above equation could not exist, so we will apply numerical methods to solve differential equations. Numerical methods provide a practical and versatile approach to solving differential equations where exact solutions are challenging or impossible. For this process, we chose two conditions. The first initial condition of IC-I is and second one condition is IC-II [67]-[70] is

$$\eta^{\hat{1}}(b) = 1, \frac{d\eta^{\hat{1}}(b)}{d\tau} = 0.$$

Figures 1, 2, and 3 show the radial component of the geodesic deviation vector of RMSBH with ICI as a function of  $r$  for different values of  $\Lambda$ ,  $a$  and  $b$ . The value of  $\eta^{\hat{i}}(r)$  decreases with increasing the value of  $\Lambda$  (cosmological constant) but increases with increasing the value of  $\Lambda$ , (rindler acceleration). The geodesic

deviation path is infinitesimally closer to each other when the radius and  $b$  are increased. As in Figures 7, 8, and 9, we plot the angular component of the geodesic deviation vector of RMSBH with ICII as a function of  $r$  for different values of  $\Lambda$ ,  $a$  and  $b$ . The value of  $\eta^i(r)$  increases with increasing the value  $\Lambda$  and monotonically decreases when increasing the value of  $\Lambda$  as well as  $b$ . The geodesic deviation paths are infinitesimally closer as the radius increases, and the angular geodesic deviation vector compresses in the angular direction in Fig. 9.

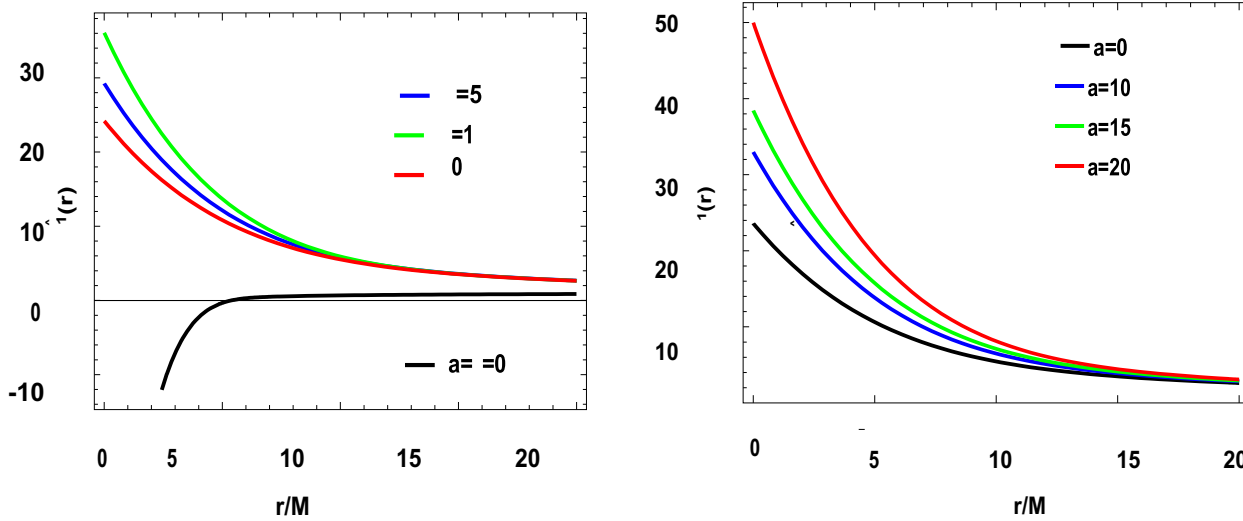


**Figure 1 & 2 :**  $\eta^i(r)$  Verses  $r$  for  $M = 1, a = 2, b = 10$  and  $\Lambda = 0$  to 15. &  $\eta^i(r)$  verses  $r$  for  $M = 1, \Lambda = 2, b = 10$  and  $a = 0$  to 20.

Figures 4 and 5 (the dial component of geodesic deviation) show converse behavior compared to Figures 7 and 8 (the angular component of geodesic deviation).

#### 4. Conclusions

We explore the geodesic deviation and tidal force impacts of the RMSBH. To assess the radial and angular tidal forces influencing a particle falling radially toward a BH, we construct the curvature tensor within the context of a tetrad basis. The variation in Newtonian radial acceleration for a test particle moving in RMSBH along the radial direction with  $\Lambda$  and  $a$  parameters. The cosmological constant  $\Lambda$  and rindler parameter  $a$  enhance the absolute value of the Newtonian radial acceleration.

The variation of radial tidal force with the  $\Lambda$  parameter, The radial tidal forces increase with the value of  $\Lambda$ , but show a decreasing curve to smooth the path along a radial direction. The variation of angular tidal force with respect to  $\Lambda$  (cosmological constant) shows increasing behaviour and gradually decreases to a smooth curve when increasing the radius. The angular tidal force sharply decreases with an increase in the value of  $a$ , and also the tidal forces compress in angular direction until  $r \rightarrow \infty$ .

For various values of  $\Lambda$ ,  $a$  and  $b$ , the radial component of the geodesic deviation vector of RMSBH with ICI as a function of  $r$ . When  $\Lambda$  (the cosmological constant) is increased, the value of  $\eta^i(r)$  falls, while  $a$  (rindler acceleration) grows. When  $b$  and radius are increased, the geodesic deviation route becomes infinitesimally closer to one another.

---

For various values of  $\Lambda$ ,  $a$  and  $b$ , the angular component of the geodesic deviation vector of RMSBH with ICII as a function of  $r$ . As the value of  $\Lambda$  increases, so does the value of  $\eta^{\hat{i}}(r)$ , which decreases monotonically as both  $b$  and  $\Lambda$  grow. As the radius increases, the geodesic deviation paths become infinitesimally closer to one another, and the angular geodesic deviation vector compresses in the direction of angular deviation.



**References**

1. S. Chandrasekhar, *Journal of Astrophysics and Astronomy* 5, 3 (1984).
2. V. Sahni, *Dark Matter and Dark Energy*, edited by E. Papantonopoulos (Springer Berlin Heidelberg, Berlin, Heidelberg, 2005) pp. 141179.
3. D. N. Spergel, *Science* 347, 1100 (2015).
4. P. J. E. Peebles and B. Ratra, *Rev. Mod. Phys.* 75, 559 (2003).
5. E. Oks, *New Astronomy Reviews* 93, 101632 (2021).
6. G. Bertone and D. Hooper, *Rev. Mod. Phys.* 90, 045002 (2018).
7. C. D. Hoyle et al., *Phys. Rev. Lett.* 86, 1418 (2001).
8. D. O. Sabulsky et al., *Phys. Rev. Lett.* 123, 061102 (2019).
9. S. Weinberg, *Gravitation and Cosmology* (John Wiley and Sons, Inc, 1972).
10. E. Poisson and C. M. Will, *Gravity* (Cambridge University Press, Cambridge, 2014).
11. C. M. Will, *Living Reviews in Relativity* 17, 1 (2014).
12. C. W. F. Everitt et al., *Phys. Rev. Lett.* 106, 221101 (2011).
13. I. Shapiro, in *General Relativity and Gravitation, 1989*, edited by N. Ashby, D. F. Bartlett, and W. Wyss (1990) p.313.
14. T. L. Smith et al., *Phys. Rev. D* 77, 024015 (2008).
15. F. D. Marchi and G. Cascioli, *Classical and Quantum Gravity* 37, 095007 (2020).
16. R. A. Hulse and J. H. Taylor, *Astrophysical Journal letters* 195, 51 (1975).
17. H. Stairs, *Living Reviews in Relativity* 6, 1 (2003).
18. M. Kramer et al., *science* 314, 97 (2006). 12
19. H. Hu, *Gravity Tests with Pulsars Using New-Generation Radio Telescopes*, Ph.D. thesis, Universitäts-und Landesbibliothek Bonn (2023).
20. N. Yunes and D. N. Spergel, *Phys. Rev. D* 80, 042004 (2009).
21. E. Berti et al., *Classical and Quantum Gravity* 32, 243001 (2015).
22. M. Ishak, *Living Reviews in Relativity* 22, 1 (2019).
23. S. E. Gralla, *Phys. Rev. D* 103, 024023 (2021).
24. J. P. Uzan, *Philosophical Transactions of the Royal Society A: Mathematical, Physical and Engineering Sciences* 369, 5042 (2011).
25. T. Padmanabhan, *Phys.Rep.* 380, 235 (2003).
26. E. Hackmann and C. Lammerzahl, *Phys. Rev. D* 78, 024035 (2008),
27. D. Grumiller, *Model for gravity at large distances*, *Phys. Rev. Lett.* 105 (2010) 211303.
28. J. Sultana, D. Kazanas, *Bending of light in modified gravity at large distances*, *Phys. Rev. D* 85 (2012) 081502.
29. D. Grumiller, F. Preis, *Rindler force at large distances*, *Internat. J. Modern Phys. D* 20 (2011) 2761.
30. S. G. Turyshev, V.T. Toth, G. Kinsella, S.C. Lee, S.M. Lok, J. Ellis, *Support for the thermal origin of the pioneer anomaly*, *Phys. Rev. Lett.* 108 (2012) 241101.
31. D. Grumiller, *Erratum: Model for gravity at large distances*, *Phys. Rev. Lett.* 106 (2011) 039901.
32. H. N. Lin, M.H. Li, X. Li, Z. Chang, *Galaxy rotation curves in the Grumillers modified gravity*, *Mon. Not. R. Astron. Soc.* 430 (2013) 450.
33. F. Walter, et al., *Things: The HI nearby galaxy survey*, *Astron. J.* 136 (2008) 2563.
34. J. Mastache, J. L. Cervantes-Cota, A. de la Macorra, *Testing modified gravity at large distances with the HI nearby galaxy surveys rotation curves*, *Phys. Rev. D* 87 (2013) 063001.
35. L. Cervantes-Cota, J.A. Gomez-Lopez, *Testing Grumillers modified gravity at galactic scales*, *Phys. Lett. B* 728 (2014) 537.
36. S. F. Mirekhtiary, I. Sakalli, *Hawking radiation of Grumiller black hole*, *Commun. Theor. Phys.* 61 (2014) 558.
37. Sakalli, S. F. Mirekhtiary, *Spectroscopy of rindler modified Schwarzschild black hole*, *Astrophys. Space Sci.* 350 (2014) 727.
38. [38] I. Sakalli, . Ovgun, *Hawking radiation and deflection of light from Rindler modified 13 Schwarzschild black hole*, *Europhys. Lett.* 118 (2017) 60006.
39. B. F. Schutz, *A First Course in General Relativity* (Cambridge University Press, Cambridge, 1985).

40. J. B. Hartle, *Gravity: An Introduction to Einsteins General Relativity* (Addison-Wesley, San Francisco, 2002).
41. S. T. Hong, Y. W. Kim, Y. J. Park, Tidal effects in Schwarzschild black hole in holographic massive gravity. *Phys. Lett. B* 811, 135967 (2020).
42. M. Abdel-Megied, R.M. Gad, On the singularities of ReissnerNordstrm space-time. *Chaos Solitons Fractals* 23, 313 (2005).
43. L. C. B. Crispino, A. Higuchi, L.A. Oliveira, E.S. de Oliveira, Tidal forces in ReissnerNordstrmm spacetimes. *Eur. Phys. J. C* 76, 168(2016).
44. H. C. D. L. Junior, L.C.B. Crispino, Tidal forces in the charged Hayward black hole spacetime. *Int. J. Mod. Phys. D* 29, 2041014 (2020).
45. M. Sharif, S. Sadiq, Tidal effects in some regular black holes. *J. Exp. Theor. Phys.* 126, 194 (2018).
46. M. U. Shahzad, A. Jawad, Tidal forces in Kiselev black hole. *Eur. Phys. J. C* 77, 372 (2017).
47. Goel, R. Maity, P. Roy, T. Sarkar, Tidal forces in naked singularity backgrounds. *Phys. Rev. D* 91, 104029 (2015).
48. J. A. Wheeler, Mechanisms for jets, in *Proceedings of a Study Week on Nuclei of Galaxies*, ed. by D. J. K. OConnell, pp 549567 (1971).
49. M. Kesden, Tidal-disruption rate of stars by spinning supermassive black holes. *Phys. Rev. D* 85, 024037 (2012).
50. J. P. Luminet, J.A. Marck, Tidal squeezing of stars by Schwarzschild black holes. *Mon. Not. R. Astron. Soc.* 212, 57 (1985).
51. L. G. Fishbone, The relativistic Roche problem. I. Equilibrium theory for a body in equatorial, circular orbit around a Kerr black hole. *Astrophys. J.* 185, 43 (1973).
52. M. Ishii, M. Shibata, Y. Mino, Black hole tidal problem in the Fermi normal coordinates. *Phys. Rev. D* 71, 044017 (2005).
53. T. W. S. Holoien et al., Discovery and early evolution of ASASSN19bt, the first TDE detected by TESS. *Astrophys. J.* 883, 17 (2019).
54. H. C. D. L. Junior, L. C. B. Crispino, A. Higuchi, On-axis tidal forces in Kerr spacetime. *Eur. 14 Phys. J. Plus* 135, 334 (2020).
55. [55] G. Abbas and M. Asgher, Tidal effects in AdS charged torus-like black hole, *MPLA* 37, 2250198 (2022).
56. [56] G. Abbas and M. Asgher, Tidal effect in charged black hole enclosed by thin accretion disc in Rastall gravity, *New Astronomy* 99, 101967 (2023).
57. G. Abbas and M. Asgher, Tidal effects in black hole of non-linear electrodynamic field, *Phys. Scr.* 98 045010 ( 2023).
58. D. Grumiller, Model for gravity at large distances, *Phys. Rev. Lett.* 105 (2010) 211303.
59. D. Grumiller, W. Kummer, D. V. Vassilevich, Dilaton gravity in two dimensions, *Phys. Rep.* 369 (2002) 327.
60. [60] V. P. Frolov, I. D. Novikov, *Black Hole Physics: Basic Concepts and New Developments*, Kluwer Academic Publishers, London, 1998.
61. G. Riess, et al., Observational evidence from supernovae for an accelerating universe and a cosmological constant, *Astron. J.* 116 (1998) 1009.
62. J. D. Anderson, P. A. Laing, E. L. Lau, A. S. Liu, M.M. Nieto, S.G. Turyshev, Study of the anomalous acceleration of Pioneer 10 and 11, *Phys. Rev. D* 65 (2002)082004.
63. M. Milgrom, A modification of the Newtonian dynamics as a possible alternative to the hidden mass hypothesis, *Astrophys. J.* 270 (1983) 365370.
64. C. W. Misner, K. S. Thorne, and J. A. Wheeler, *Gravitation* (Freeman, San Francisco, 1973).
65. R. D Inverno, *Introducing Einsteins Relativity* (Clarendon Press, Oxford, 1992).
66. M. P. Hobson, G. Efstathiou, A.N. Lasenby, *General Relativity An Introduction for Physicists* (Cambridge University Press, Cambridge,2006).
67. Gomboc and A. Cadež *Ap. J.* 625, 278 (2005).
68. M. Brassart and J. P. Luminet *A. A* 481, 259 (2008). [69] P. Hut *A. A* 92, 167 (1980).
69. P. Hut *A. A* 99, 126 (1981). [71] P. Hut *A. A* 110, 37 (1982).